



Paleoceanography and Paleoclimatology

RESEARCH ARTICLE

10.1029/2018PA003362

Key Points:

- Radiative forcing by CO₂ linearly related to pH change, second carbonate system parameter is not required
- Using the boron isotope proxy, uncertainty of seawater boron isotopic composition has weaker effect on pH change than absolute pH
- Short time slices of high-resolution boron isotope data better suited to reconstruct climate forcing than long-term, low-resolution records

Correspondence to:

M. P. Hain,
mhain@ucsc.edu

Citation:

Hain, M. P., Foster, G. L., & Chalk, T. (2018). Robust constraints on past CO₂ climate forcing from the boron isotope proxy. *Paleoceanography and Paleoclimatology*, 33, 1099–1115. <https://doi.org/10.1029/2018PA003362>

Received 13 MAR 2018

Accepted 12 SEP 2018

Accepted article online 17 SEP 2018

Published online 27 OCT 2018

Robust Constraints on Past CO₂ Climate Forcing From the Boron Isotope Proxy

M. P. Hain¹ , G. L. Foster² , and T. Chalk² 

¹Earth and Planetary Sciences, University of California, Santa Cruz, CA, USA, ²Ocean and Earth Sciences, University of Southampton, Southampton, UK

Abstract The atmospheric concentration of the greenhouse gas carbon dioxide, CO₂, is intimately coupled to the carbon chemistry of seawater, such that the radiative climate forcing from CO₂ can be changed by an array of physical, geochemical, and biological ocean processes. For instance, biological carbon sequestration, seawater cooling, and net CaCO₃ dissolution are commonly invoked as the primary drivers of CO₂ change that amplify the orbitally paced ice age cycles of the late Pleistocene. Based on first-principle arguments with regard to ocean chemistry, we demonstrate that seawater pH change (Δ pH) is the dominant control that effectively sets CO₂ radiative forcing (Δ F) on orbital timescales, as is evident from independent late Pleistocene reconstructions of pH and CO₂. In short, all processes relevant for CO₂ on orbital timescales, including temperature change, cause pH to change to bring about fractional CO₂ change so as to yield a linear relationship of Δ pH to CO₂ climate forcing. Further, we show that Δ pH and CO₂ climate forcing can be reconstructed using the boron isotope pH proxy more accurately than absolute pH or CO₂, even if seawater boron isotope composition is poorly constrained and without information on a second carbonate system parameter. Thus, our formalism relaxes otherwise necessary assumptions to allow the accurate determination of orbital timescale CO₂ radiative forcing from boron isotope pH reconstructions alone, thereby eliminating a major limitation of current methods to estimate our planet's climate sensitivity from the geologic record.

1. Introduction

Atmospheric carbon dioxide (CO₂) is a greenhouse gas that causes a radiative forcing of +3.7 W/m² per CO₂ doubling (e.g., Byrne & Goldblatt, 2014; Myhre et al., 1998), and changes in CO₂ have been identified as important drivers of climate change in the geologic past (e.g., Shakun et al., 2012; Sigman et al., 2010; Zachos et al., 2008). Reconstructing CO₂ change and its associated climate forcing from the geologic record is important for our understanding of the history of physical, chemical, and biological changes in the Earth system. In particular, reconstructing the relationships between CO₂ climate forcing and climatic parameters such as temperature, ice sheet mass, and sea level provides valuable insights into the couplings and feedbacks operating within Earth's climate system and their dependence on the background climate state (e.g., Chalk et al., 2017; Martinez-Boti et al., 2015). In the context of ongoing warming dominated by anthropogenic carbon emissions Earth's climate sensitivity, the average temperature change per CO₂ doubling, has become a contested parameter of central importance (IPCC, 2014). Given reconstructions of CO₂ and global temperature change, it is possible to estimate climate sensitivity from the geologic record (e.g., PALEOSENS Project Members, 2012; Rohling et al., 2018), offering an important test for estimates based purely on computational climate models (e.g., Andrews et al., 2012) and helping to refine estimates of today's climate sensitivity (e.g., Goodwin et al., 2018; Knutti et al., 2017). This is particularly true for past climate intervals that are warmer than the present, implicitly integrating all known and unknown climate feedbacks operating in the Earth system. However, other than for the last 800 thousand years when ice core records accurately capture CO₂ change and its climate forcing, most methods used to reconstruct CO₂ in the more distant and typically warmer-than-present geological past are indirect and generally associated with substantial stochastic and systematic uncertainties (e.g., Breecker et al., 2010; Foster & Rae, 2016; Franks et al., 2014; Hemming & Hönisch, 2007; Pagani, 2014; Royer, 2006). These systematic uncertainties in reconstructing atmospheric CO₂ need to be overcome if we hope to robustly constrain the mechanisms of climate change in general and climate sensitivity in particular from the geologic record.

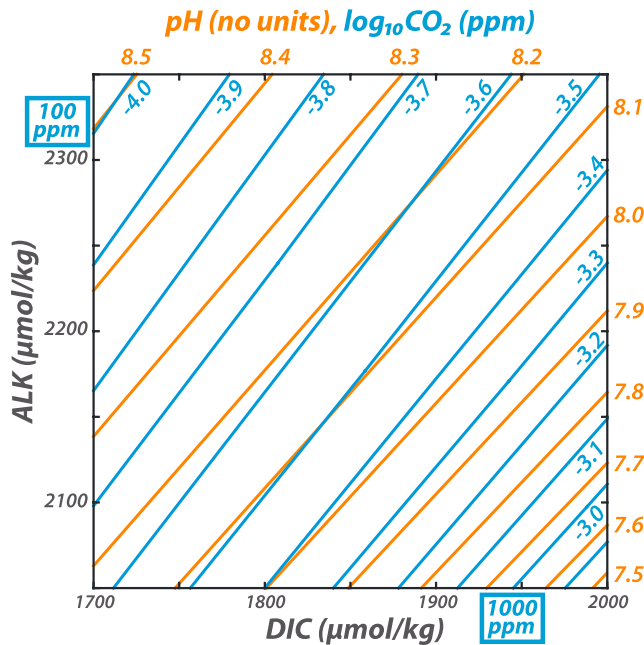


Figure 1. Illustration of the tight coupling between CO₂ and pH. Across a wide range of dissolved inorganic carbon (DIC) and alkalinity (ALK) concentrations contours of constant pH and constant CO₂ are broadly aligned, with similar spacing between pH and log₁₀CO₂ contours. This suggests that H⁺ and CO₂ are approximately proportional across the plotted field of DIC and ALK, which covers more than an order of magnitude CO₂ change. In this study we formally explore the mechanisms and implications of the pH-CO₂ relationship in the context of our ability to reconstruct past CO₂ climate forcing.

It is well established that pH and CO₂ are closely tied by seawater carbonate chemistry (Figure 1), with closely aligned contours of constant pH and CO₂. We note further that the spacing of contours of constant pH and log₁₀CO₂ is very similar, which suggests a near linear relationship between H⁺ and CO₂. In this study we formally examine this relationship in the context of the boron isotope pH proxy. Our main point is to greatly relax assumptions that are currently required in the reconstruction of CO₂ radiative forcing based on the boron isotope pH proxy, thereby also eliminating a significant source of unnecessary uncertainty and facilitating the exploration of climate sensitivity throughout at least the last 65 million years.

This manuscript is organized as follows. First, in section 2, we lay out the theory that underpins our formalism of the relationship between pH change (ΔpH) and CO₂ radiative forcing (ΔF). Then we use mathematical derivations and numerical solutions to demonstrate the reason why ΔpH and ΔF change in unison regardless of whether these changes are caused by the addition/removal of carbon and CaCO₃ or increases/decreases in temperature. Second, in section 3, we show that the observed relationship of ΔpH change and independently reconstructed ΔF from ice core measurements of the last 260 thousand years indeed agrees with our theory, that ΔpH can be robustly reconstructed using the boron isotope pH proxy even if the boron isotopic composition of seawater is poorly constrained, and that applying our formalism can yield useful constraints on climate sensitivity. Finally, in section 4, we critically assess the caveats and assumptions of our formalism, discussing specifically when our approach should not be applied and considerations for the sampling strategy best suited to constrain ΔF and climate sensitivity from the geologic record. Overall, our study suggests that it is possible to use the boron isotope pH proxy to derive

robust estimates of past ΔpH , ΔF , and climate sensitivity even if (a) the cause of past CO₂ change is unknown, (b) the boron isotopic composition of seawater is poorly constrained, and (c) without information on a second carbonate system parameter.

2. Formalism and Derivations

If the goal is to estimate absolute CO₂ concentrations based on reconstructed pH, then there are no shortcuts to the established formalism (e.g., Zeebe & Wolf-Gladrow, 2001), which requires, for example, accurate measurement of boron isotopic composition of planktonic foraminifera, correction for vital effects, temperature and salinity reconstructions, accurate knowledge of seawater boron isotopic composition, equilibrium constant corrections for seawater major ion change, and a fully independent estimate of a second carbon chemistry parameter. The latter point especially is a major problem because no method currently exists to reconstruct seawater carbon concentration or alkalinity and their changes over geologic time. However, to calculate CO₂ climate forcing (ΔF , in W/m²), we do not need to know absolute CO₂, or even absolute CO₂ change, but only fractional CO₂ change (i.e., the change in the logarithm of CO₂, $\Delta\log\text{CO}_2$):

$$\Delta F = \alpha_{2\times\text{CO}_2} \times \Delta \log_2 \text{CO}_2 = \frac{\alpha_{2\times\text{CO}_2}}{\log_{10} 2} \times \Delta \log_{10} \text{CO}_2 \quad (1)$$

where $\alpha_{2\times\text{CO}_2}$ is the sensitivity of the radiative balance per CO₂ doubling, $\Delta\log_2\text{CO}_2$. For large parts of the subtropical and tropical ocean the carbon and acid/base chemistry of surface waters remain near equilibrium with atmospheric CO₂ because of shallow mixed layer depth and strong density stratification that greatly restricts exchange between equilibrating surface water and underlying waters (Rodenbeck et al., 2013; Takahashi et al., 2002, 2009). Assuming that surface water CO₂ partial pressure in these regions tracks

atmospheric CO₂, the fractional CO₂ change relative to a reference, $\Delta \log_{10} \text{CO}_2 = [\log_{10} \text{CO}_2] - [\log_{10} \text{CO}_2]_{\text{reference}}$, can be expressed as follows:



$$\text{CO}_2 = \frac{\text{H}^+ \times \text{HCO}_3^-}{K_0 \times K_1} \quad (2b)$$

$$\log_{10} \text{CO}_2 = \log_{10} \text{HCO}_3^- + \text{p}K_0 + \text{p}K_1 - \text{pH} \quad (2c)$$

$$\Delta \log_{10} \text{CO}_2 = \Delta \log_{10} \text{HCO}_3^- + \Delta \text{p}K_0 + \Delta \text{p}K_1 - \Delta \text{pH} \approx - \Delta \text{pH} \quad (2d)$$

Equation (2a) is the chemical equation for the equilibrium of reversible CO₂ hydration and deprotonation to bicarbonate and free proton, and Equation (2b) quantitatively describes this standard relationship between CO₂ and seawater carbonate chemistry. To yield a distinct pH term in Equation (2c), we take the logarithm of equation (2b). To write Equation (2d) as an expression that relates fractional CO₂ change ($\Delta \log_{10} \text{CO}_2$) to pH change (ΔpH), we take the difference between two states of carbonate chemistry written in the form of equation (2c). The other terms appearing in equations (2a)–(2d) are the bicarbonate concentration HCO₃[−], and the carbonate chemistry equilibrium constants K₀ and K₁. Bicarbonate is by far the dominant form of carbon and therefore approximates the total dissolved inorganic carbon (DIC) concentration. The carbonate system equilibrium constants change with temperature, salinity, and seawater major ion composition.

The basic argument of this study is that the right-hand side of equation (2d) is dominated by ΔpH , and thus past fractional CO₂ change may be usefully constrained by reconstructing pH change alone. If so, combining equations (1) and (2a)–(2d) yields a linear relationship between pH change (ΔpH) and climate forcing from atmospheric CO₂ change (ΔF):

$$\Delta F \approx 3.7 \frac{W}{m^2} \times \Delta \log_2 \text{H}^+ = -12.3 \frac{W}{m^2} \times \Delta \text{pH} \quad (3)$$

Our formalism posits that fractional CO₂ change is dominantly caused by pH change, without specifying the set of processes responsible for the pH change and without assessing the magnitude of the error incurred by using that approximation. In the following sections we demonstrate that both carbon and CaCO₃ addition/removal (section 2.1) as well as the temperature effects on CO₂ solubility and equilibrium constants (section 2.2) indeed cause very similar fractional change in H⁺ and CO₂, thereby yielding a linear relationship between ΔpH and ΔF as posited by our formalism.

2.1. Carbon and CaCO₃ Addition/Removal

The carbon chemistry of seawater is tied to the overall concentration of DIC and the relative excess of dissolved bases over acids, alkalinity (ALK). Biological production or respiration of soft-tissue organic matter mainly removes or adds carbon to seawater, with only a very small effect on ALK. Conversely, biological production of CaCO₃ and its dissolution act to change ALK and DIC in a strict 2-to-1 ratio. The formalism outlined above presumes that the addition or removal of both DIC and CaCO₃ causes most of its effect on CO₂ by changing the partitioning of DIC among carbonic acid, bicarbonate ion, and carbonate ion, as reflected by pH change, rather than by changing the total dissolved carbon concentration itself (i.e., little change in the HCO₃[−] term in equations (2a)–(2d)). To assess the validity of this assertion, we impose DIC and CaCO₃ addition/removal and use a carbonate chemistry solver to calculate the resulting changes in pH and CO₂ (Figure 2; see panel a for DIC perturbation and panel b for CaCO₃ perturbation). Our formalism posits that the fractional change in H⁺ equals the fractional change in CO₂, such that $\Delta \log_{10} \text{CO}_2$ equals ΔpH (i.e., solid black line in Figure 2d). When cross plotting calculated pH and CO₂ (on a logarithmic axis), we find that both DIC and CaCO₃ addition/removal result in a linear pH-to- $\log_{10} \text{CO}_2$ relationship, but the slope of that relationship is about 30% steeper for DIC and about 10% less steep for CaCO₃ addition/removal than posited by our formalism. That is, while our basic formalism presumes an equal magnitude of ΔpH and $\Delta \log_{10} \text{CO}_2$ (e.g., equations (2a)–(2d)), the consistent deviations from that expectation for DIC and CaCO₃ addition/removal

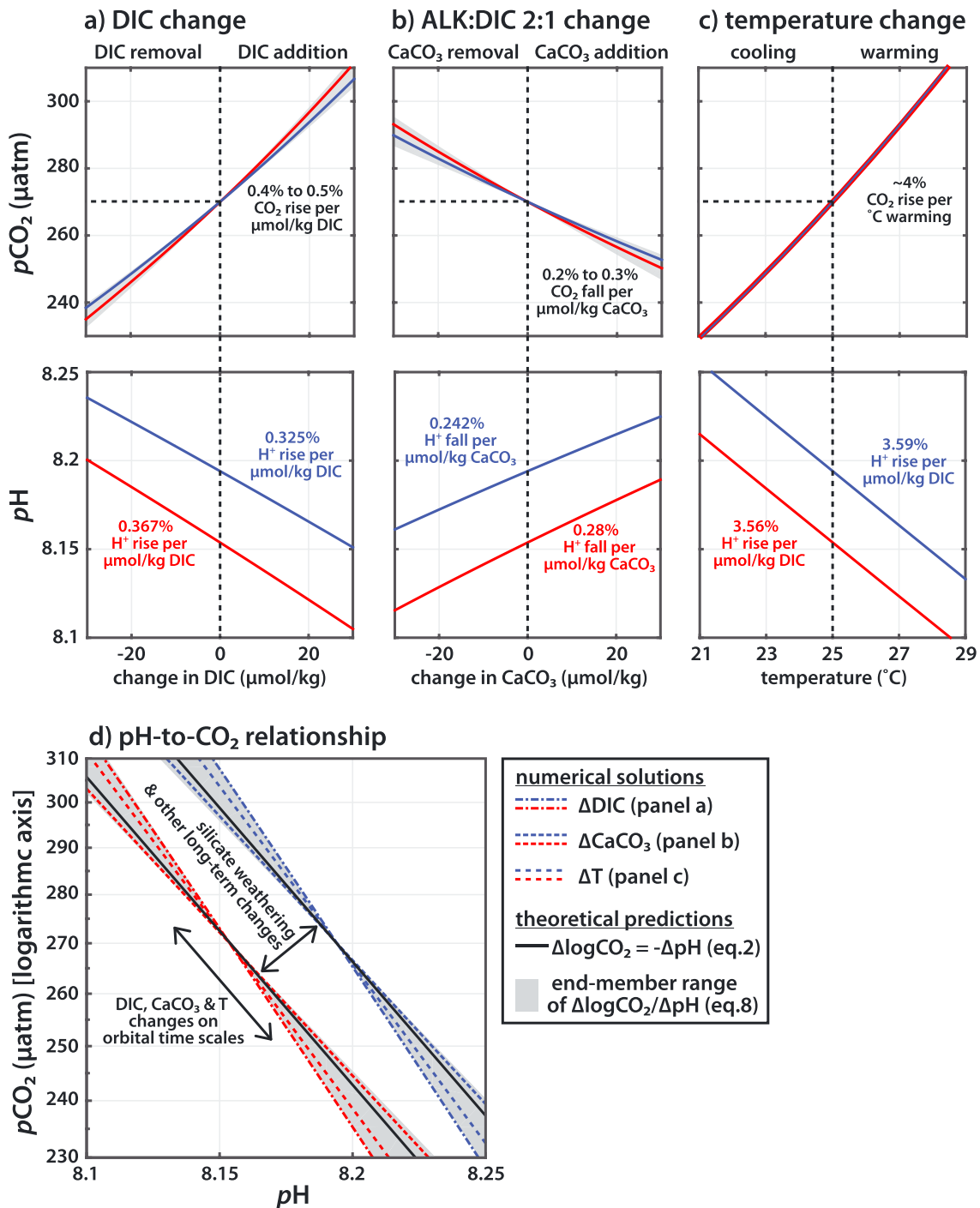


Figure 2. Sensitivity of CO_2 partial pressure and pH to incremental perturbation of (a) dissolved inorganic carbon (DIC), (b) CaCO_3 with an alkalinity-to-DIC ratio of 2:1, (c) temperature, and (d) the relationships between CO_2 and pH of experiments (a) to (c). Blue and red lines indicate two separate experiments both with an initial CO_2 of $270 \mu\text{atm}$ but with initial DIC of $1,800 \mu\text{mol/kg}$ and $2,000 \mu\text{mol/kg}$, respectively. The black lines in (d) correspond to the pH- CO_2 relationship predicted from equations (2a)–(2d) (solid) and the numerical solutions as shown in panels (a) to (c) (dashed). The purpose of this figure is to demonstrate that fractional changes in CO_2 and H^+ are nearly equal (a–c), so as to yield ΔpH -to- $\Delta\text{log}_{10}\text{CO}_2$ relationships close to -1 -to- 1 (d).

span an end-member $\Delta\text{log}_{10}\text{CO}_2/\Delta\text{pH}$ range of about $-1.3:1$ and $-0.9:1$ that needs to be propagated when using equation (3) to infer CO_2 climate forcing from pH change.

To clarify why DIC and CaCO_3 addition/removal cause $\Delta\text{log}_{10}\text{CO}_2/\Delta\text{pH}$ that deviates from unity and to demonstrate that these deviations are robust and expected it is useful to consider, the formal

mathematical expressions of CO_2 change in response to a DIC perturbation (i.e., δ_C) and a CaCO_3 perturbation (i.e., δ_{CaCO_3}), respectively, at constant temperature and salinity (i.e., no change in the equilibrium constants; see also section 2.2 for changing equilibrium constants in response to temperature change). That is, we wish to derive the partial derivatives of equilibrium CO_2 and equilibrium H^+ , which depend on bicarbonate ion (HCO_3^-) and carbonate ion (CO_3^{2-}) concentration:

$$\text{CO}_2 = \frac{\text{H}^+ \times \text{HCO}_3^-}{K_0 \times K_1} \quad (4a)$$

$$\text{H}^+ = \frac{K_2 \times \text{HCO}_3^-}{\text{CO}_3^{2-}} \quad (4b)$$

In order to write the partial derivatives of CO_2 and H^+ , we need to know the bicarbonate and carbonate ion partial derivatives to incremental chemical change, and we use the CPF (carbonate proton fraction) notation of Hain et al. (2015) to keep our expressions concise. CPF equates to the fraction of total seawater buffering that is due to the bicarbonate/carbonate ion buffer (i.e., seawater CPF of about -0.65 means that per unit of acid added carbonate ion is reduced and bicarbonate increased by 0.65 units):

$$\frac{\delta \text{CO}_3^{2-}}{\delta C} = \text{CPF} \approx \frac{-1}{1 + \text{B(OH)}_4^- / \text{CO}_3^{2-}} \sim -0.65 \quad (5a)$$

$$\frac{\delta \text{HCO}_3^-}{\delta C} = 1 - \text{CPF} \quad (5b)$$

$$\frac{\delta \text{CO}_3^{2-}}{\delta \text{ALK}} = -\text{CPF} \quad (5c)$$

$$\frac{\delta \text{HCO}_3^-}{\delta \text{ALK}} = \text{CPF} \quad (5d)$$

The partial derivatives of H^+ and CO_2 with respect to small perturbations of DIC and ALK (δ_C and δ_{ALK}) are obtained using the quotient and product rule, respectively, and substituting equations (5a)–(5d) to take the place of the bicarbonate and carbonate ion partial derivatives:

$$\frac{\delta_C \text{H}^+}{\delta C} = \frac{(1 - \text{CPF}) \times K_2}{\text{CO}_3^{2-}} - \frac{\text{CPF} \times K_2 \times \text{HCO}_3^-}{(\text{CO}_3^{2-})^2} \quad (6a)$$

$$\frac{\delta_{\text{ALK}} \text{H}^+}{\delta \text{ALK}} = \frac{(\text{CPF}) \times K_2}{\text{CO}_3^{2-}} - \frac{-\text{CPF} \times K_2 \times \text{HCO}_3^-}{(\text{CO}_3^{2-})^2} \quad (6b)$$

$$\frac{\delta_C \text{CO}_2}{\delta C} = \left\{ \frac{\delta \text{HCO}_3^-}{\delta C} \times \frac{\text{H}^+}{K_0 \times K_1} \right\} + \left[\frac{\delta \text{H}^+}{\delta C} \times \frac{\text{HCO}_3^-}{K_0 \times K_1} \right] = \left(\{1 - \text{CPF}\} + \left[1 - \text{CPF} - \frac{\text{H}^+}{K_2} \text{CPF} \right] \right) \times \frac{\text{CO}_2}{\text{HCO}_3^-} \quad (6c)$$

$$\frac{\delta_{\text{ALK}} \text{CO}_2}{\delta \text{ALK}} = \left\{ \frac{\delta \text{HCO}_3^-}{\delta \text{ALK}} \times \frac{\text{H}^+}{K_0 \times K_1} \right\} + \left[\frac{\delta \text{H}^+}{\delta \text{ALK}} \times \frac{\text{HCO}_3^-}{K_0 \times K_1} \right] = \left(\{\text{CPF}\} + \left[\text{CPF} + \frac{\text{H}^+}{K_2} \text{CPF} \right] \right) \times \frac{\text{CO}_2}{\text{HCO}_3^-} \quad (6d)$$

The partial derivative of H^+ and CO_2 with respect to small perturbation of CaCO_3 (i.e., δ_{CaCO_3}) is simply the sum of equations (6a)/(6b) and (6c)/(6d) weighted by the 2:1 stoichiometric ALK-to-DIC ratio of CaCO_3 :

$$\frac{\delta_{\text{CaCO}_3} \text{H}^+}{\delta \text{CaCO}_3} = \frac{\delta_C \text{H}^+}{\delta C} + 2 \times \frac{\delta_{\text{ALK}} \text{H}^+}{\delta \text{ALK}} \quad (7a)$$

$$\frac{\delta_{\text{CaCO}_3} \text{CO}_2}{\delta \text{CaCO}_3} = \frac{\delta_C \text{CO}_2}{\delta C} + 2 \times \frac{\delta_{\text{ALK}} \text{CO}_2}{\delta \text{ALK}} \quad (7b)$$

To arrive at the final desired expressions of fractional CO_2 change, we separate the differential and rearrange equations (6c) and (7b):

$$\frac{\delta_C \text{CO}_2}{\text{CO}_2} = \left(\{1 - \text{CPF}\} + \left[1 - \text{CPF} - \frac{\text{H}^+}{K_2} \text{CPF} \right] \right) \times \frac{\delta \text{C}}{\text{HCO}_3^-} \quad (8a)$$

$$\frac{\delta_{\text{CaCO}_3} \text{CO}_2}{\text{CO}_2} = \left(\{1 + \text{CPF}\} + \left[1 + \text{CPF} + \frac{\text{H}^+}{K_2} \text{CPF} \right] \right) \times \frac{\delta \text{CaCO}_3}{\text{HCO}_3^-} \quad (8b)$$

Both equations relate left-hand side fractional CO₂ change (i.e., incremental CO₂ change δCO₂ divided by background CO₂) to its underlying carbon chemistry causes due to carbon addition (i.e., equation (8a): incremental carbon addition δC divided by background bicarbonate ion concentration) and CaCO₃ addition (i.e., equation (8b): incremental CaCO₃ addition δCaCO₃ divided by background bicarbonate ion concentration). The curly brackets on the right-hand side are arranged to highlight the effect of changing bicarbonate concentration, whereas the square brackets highlight the effects of changing pH.

Substituting reasonable values for H⁺/K₂ and CPF into equations (8a) and (8b), we find that the pH effect dominates over the effect of bicarbonate abundance, in the case of DIC addition by about 3.4-fold (i.e., a square bracket pH change term of 5.55 relative to the curly bracket term of 1.65 for the effect of bicarbonate abundance, equation (8a)) and in the case of CaCO₃ addition by tenfold (i.e., a square bracket pH change term of −3.55 relative to the curly bracket term of 0.35, equation (8b)). That is, the relationships between ΔpH and Δlog₁₀CO₂ are not exactly −1:1 as approximated in equation (2d), but based on equations equation (8a) and equation (8b), we estimate −1:1.3 for carbon addition/removal and −1:0.9 for CaCO₃ addition/removal (the range between these end-members is shown as gray shading in Figure 2d).

The slightly stronger and weaker than predicted CO₂-to-pH relationships for incremental DIC and CaCO₃ addition/removal, respectively, are quantitatively consistent with the carbonate chemistry solver results shown in Figure 2, underscoring on a mechanistic level that pH change caused by DIC and CaCO₃ addition/removal is the dominant driver of CO₂ change, whereas the much weaker effect of changing bicarbonate abundance is responsible for the deviation of the ΔpH-to-Δlog₁₀CO₂ relationship from the −1:1 solely pH-driven slope (i.e., solid black line in Figure 2d). Based on these deviations, if pH change is known exactly, then Δlog₁₀CO₂ and CO₂ climate forcing can be estimated to within the end-member bounds of −10% for purely CaCO₃-caused and +30% for purely DIC-caused carbon chemistry change (i.e., gray shading in Figure 1d), with any combination of these drivers yielding less bias relative to the formalism of equations (2a)–(2d) and (3). Later in the manuscript, in section 3.3, we will use this theoretically derived end-member uncertainty envelope when estimating CO₂ climate forcing from pH change.

2.2. Temperature Change

All of what is said above ignores the strong effects of temperature on the solubility of CO₂ in seawater and on the equilibrium constants that govern the deprotonation equilibria of carbonic acid and bicarbonate ion: that is, K₀, K₁, and K₂. This raises the question if temperature change associated with CO₂ climate forcing can reduce the utility of our formalism for estimating CO₂ climate forcing from reconstructed pH change. That is, does temperature change CO₂ independently of pH? To address this question, we derive the sensitivity of fractional CO₂ change to incremental change in temperature, and we use a carbonate chemistry solver to confirm that temperature change cause fractional CO₂ and H⁺ changes very close to the posited −1:1 relationship.

Analogous with the derivation of the DIC and CaCO₃ effects above, we use the product rule to arrive at the partial derivative of H⁺ and CO₂, but this time due to temperature change in absence of DIC or ALK perturbation. Since the speciation of the set concentration of carbon is constrained by the set ALK, we take the partial derivatives of bicarbonate and carbonate ion to be zero (a very good approximation) and only consider changes in the equilibrium constants and the minor species [H⁺] and (implicitly) carbonic acid:

$$\frac{\delta_T H^+}{\delta T} \cong \frac{HCO_3^-}{CO_3^{2-}} \times \frac{\delta_T K_2}{\delta T} = \frac{CO_2}{K_2} \times \frac{\delta_T K_2}{\delta T} \quad (9a)$$

$$\frac{\delta_T CO_2}{\delta T} \cong \left\{ \frac{-CO_2}{K_0 \times K_1} \times \frac{\delta_T (K_0 \times K_1)}{\delta T} \right\} + \left[\frac{CO_2}{K_2} \times \frac{\delta_T K_2}{\delta T} \right] \quad (9b)$$

To arrive at the final desired expression of fractional CO₂ change in response to temperature change, we separate the differential and rearrange equation (9b):

$$\frac{\delta_T CO_2}{CO_2} \cong \left\{ -\frac{\delta_T K_0}{K_0} - \frac{\delta_T K_1}{K_1} \right\} + \left[\frac{\delta_T K_2}{K_2} \right] \approx \left(\left\{ \frac{3\%}{^\circ C} - \frac{2.5\%}{^\circ C} \right\} + \left[\frac{3.5\%}{^\circ C} \right] \right) \times \delta T \quad (10)$$

From this approximation we find three dominant terms governing CO₂ sensitivity to incremental warming that can be described as (K₀ term) a fractional decrease in CO₂ solubility K₀ causes a fractional CO₂ increase; (K₁ term) at a given pH a fractional increase in the bicarbonate-to-carbonic acid equilibrium constant K₁ causes a fractional CO₂ decrease; and (K₂ term) constant DIC and ALK demand that the carbonate-to-bicarbonate ion ratio is nearly constant so that a fractional increase in the carbonate-to-bicarbonate ion equilibrium constant K₂ causes a fractional increase of H⁺. This latter fractional H⁺ increase, a pH decline, translates to a fractional increase in CO₂. Put a different way, the K₀ and K₁ effects (curly bracket in equation (10)) operate mainly by changing the abundance and solubility of the least abundant dissolved inorganic carbon species, carbonic acid, whereas the K₂ effect (square bracket) changes the pH at which the main seawater acid/base buffer, bicarbonate-to-carbonate ion, is at equilibrium.

When using a carbonate chemistry solver, we find the net sensitivity of CO₂ to temperature change (at constant DIC and ALK) is about a 4% increase per degree of warming (Figure 2c), which agrees very well with the sum of the three individual effects isolated in equation (10). Likewise, the carbonate chemistry solver yields about 3.5% H⁺ increase per degree of warming, fully consistent with the square bracket K₂ term in equation (10). All three terms in equation (10) have a similar magnitude, but the two terms (K₀, K₁) that operate through carbonic acid have opposite sign and nearly cancel each other, whereas the K₂ term that operates through pH is unopposed. For this reason, the pH-driven CO₂ change (square bracket) is sevenfold greater than the CO₂ change driven by the combination of carbonic acid solubility and deprotonation (curly bracket; equation (10)). Thus, by fortuitous coincidence, the sensitivities of fractional H⁺ change and fractional CO₂ change to incremental warming or cooling is approximately the same (Figure 2c), yielding a −1:1.14 ΔpH-to-Δlog₁₀CO₂ relationship that is close to the −1:1 approximation in equation (2d), and it falls within the end-member range of DIC and CaCO₃ addition/removal (see section 2.1). That is to say, the net effect of temperature on fractional CO₂ change can be estimated from pH change in the very same way as CO₂ change caused by the addition or removal of DIC and CaCO₃ (Figure 2c and 2d).

3. Validation and Applications

3.1. Relationship of pH and Ice Core CO₂

Our formalism, equation (3), suggests that on orbital timescales there should be a linear relationship between CO₂ radiative climate forcing and pH change of the well-equilibrated subtropical ocean surface, with the slope of that relationship effectively set by the independently determined (e.g., Byrne & Goldblatt, 2014; Myhre et al., 1998) radiative effect per CO₂ doubling. We test this assertion by combining the continuous late Pleistocene ice core atmospheric CO₂ record with overlapping boron isotope measurements on planktonic foraminifera. Recently collected data from ODP Site 999 (Chalk et al., 2017) offers the unique opportunity to rigorously test the theory over the last 260 thousand years.

Ice core CO₂ data are precise, accurate (e.g., Bereiter et al., 2015), and using equation (1) can be easily converted into climate forcing, Δ*F*. Foraminiferal boron isotope data can be used to reconstruct surface pH given auxiliary knowledge of temperature and bulk seawater boron isotopic composition (Foster & Rae, 2016; Hemming & Hanson, 1992; Spivack et al., 1993; Vengosh et al., 1991; Zeebe & Wolf-Gladrow, 2001). For the purpose of this proof-of-concept test we use Mg/Ca-based sea surface temperature (SST) data only to account for the temperature effect on the pH reconstruction (i.e., p*K*_b temperature dependence; using our

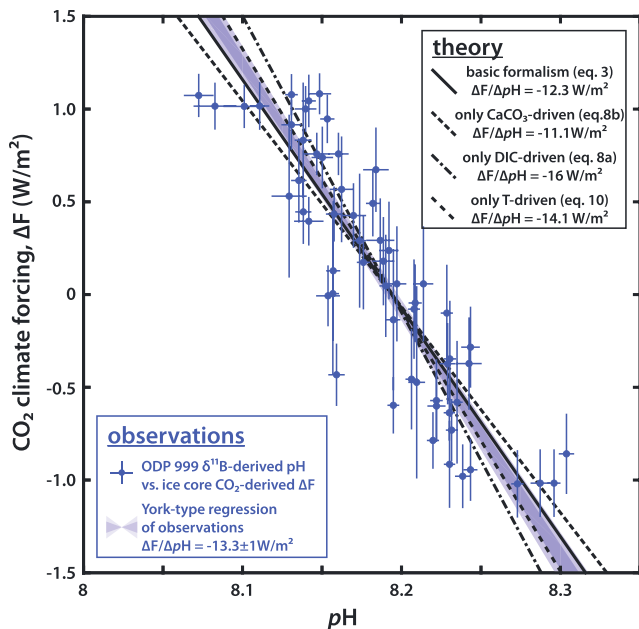


Figure 3. Relationship between CO_2 climate forcing from ice core CO_2 reconstructions and pH from boron isotope record at ODP Site 999. The regression of the data is shown as blue shading, representing the 1σ and 2σ intervals confidence intervals. The regressed slope is statistically indistinguishable from that predicted by theory (equation (3)), confirming a ΔpH -to- $\Delta\log_{10}\text{CO}_2$ relationship close to $-1:1$. The fact that the best fit regressed slope is marginally lower than theory can be taken as evidence for the relative importance in driving glacial/interglacial CO_2 change of whole ocean alkalinity changes via the open system CaCO_3 cycle. This result is consistent with modeling results (Hain et al., 2010; Toggweiler, 1999).

and light blue shading in Figure 3 represents the 1σ and 2σ envelope of the maximum likelihood model (i.e., $\Delta F/\Delta\text{pH} = -13.3 \text{ W/m}^2$; with 1σ of 0.5 W/m^2). That is, the best fitting model through the data is very close to the theoretical $\Delta F/\Delta\text{pH}$ relationship of -12.3 W/m^2 (solid black line in Figure 3) and indeed we cannot reject the null hypothesis that the data results from a strict adherence to our basic formalism (i.e., equation (3)) plus random Gaussian error. This error term can be estimated from the residuals to be 1σ of $\sim 0.32 \text{ W/m}^2$, and it corresponds to the superposition of boron isotope measurement uncertainty, age error, air/sea disequilibrium, etc.

In the above analysis we have validated our basic formalism without considering that equation (3) is a useful approximation rather than a first-principle law. As is evident from Figure 2d and equations (8a) and ((8b)(8a)) and (10) the first principle slope of the $\Delta F/\Delta\text{pH}$ relationship is $\sim 14\%$ – 30% steeper if the driving process is a change in temperature or DIC addition/removal, while it is $\sim 10\%$ less steep when caused by CaCO_3 addition/removal. In this context, we can reject the null hypothesis that overall glacial-interglacial CO_2 change and its climate forcing were exclusively driven by either biological sequestration of carbon or ocean alkalinity changes via the open system CaCO_3 cycle. This outcome is consistent with the large body of evidence that glacial cooling, carbon sequestration from the atmosphere, and upper ocean via the biological pump into the deep ocean, as well as whole ocean alkalinity increase related to transient and steady state lysocline change all contributed to ice age CO_2 drawdown (e.g., Hain et al., 2014; Martinez-Garcia et al., 2014; Sigman & Boyle, 2000; Sigman et al., 2010; Wang et al., 2017). Because the best fitting regressed slope falls between the CaCO_3 end-member on one side and the temperature and DIC end-members on the other side, we conclude that a relatively large portion of overall glacial/interglacial CO_2 change appears to have been driven by changes in whole ocean alkalinity related to transient imbalances in the ocean's open system CaCO_3 cycle, resonating with one of the earliest hypothesis to explain these changes (Broecker & Peng, 1987). All of these processes have acted at different times in the glacial progression (e.g., Hain et al., 2010), such that

formalism, we need not calculate the carbonate chemistry equilibrium constants pK_0 , pK_1 and pK_2) and we presume known modern boron isotopic composition of seawater (39.61 ‰; Foster et al., 2010), as is appropriate for the late Pleistocene given the multimillion year ocean residence time of boron (Lemarchand et al., 2002; Spivack & Edmond, 1987). The new boron isotope and Mg/Ca data (Chalk et al., 2017) that overlaps with the ice core CO_2 record was measured at the University of Southampton using established and extensively documented methods (Foster, 2008; Foster et al., 2013). The 1σ age uncertainty of the data is 1 kyr and 1.5 kyr for the for data points younger and older than 10 kyr, respectively.

To account for the significant age uncertainty of the boron isotope data when compared to the well-dated ice core data, we calculate the cumulative probability density of the ice core data within the $\pm 4\sigma$ age uncertainty interval, normalized by their respective likelihood given the age difference. This approach yields small uncertainty in CO_2 -driven ΔF at times that coincide with intervals of the ice core record with relatively constant CO_2 , and it yields large ΔF uncertainty for ages corresponding to rapid CO_2 change. That is, while the ice core CO_2 data itself is very accurate and well dated, the age uncertainty of the boron isotope data implies significant uncertainty in $\Delta F_{\text{ice-core}}$ at the time of the $\delta^{11}\text{B}$ -based reconstruction of pH. Plotting $\Delta F_{\text{ice-core}}$ as a function of the corresponding reconstructed pH yields a strong apparent negative correlation (Figure 3). We also plot the 1σ uncertainty intervals corresponding to the internal reproducibility of the underlying boron isotope measurement (horizontal error bars) as well as the 1σ of $\Delta F_{\text{ice-core}}$ corresponding to the age uncertainty the sediment samples (vertical error bars), which together can explain most of data scatter.

To determine the best fitting linear model, we use York regression (York et al., 2004), which accounts for uncertainty in both x and y. The dark

their relative contribution to CO₂ drawdown and the effective relationship between CO₂ and pH evolved with time. In this context, it seems plausible to decompose the relative contribution of DIC, alkalinity, and temperature changes to overall glacial/interglacial CO₂ change based on the regression of ΔF/ΔpH, but such analysis would require additional global carbon cycle modeling that is beyond the scope of this study. For the purpose of this work we note that the empirical ΔpH/ΔF slope falls well within the end member ΔpH/ΔF range for DIC and CaCO₃ changes, and that this range can be used to represent the uncertainty in the conversion from ΔpH to ΔF.

3.2. Seawater Boron Isotope Composition

The approach described above only requires a record of past pH changes to reconstruct CO₂ climate forcing, thereby making independent knowledge of background ocean carbon concentration (DIC) and temperature for the purpose of calculating the carbon chemistry equilibrium constants K₀, K₁, and K₂, unnecessary. However, to reconstruct pH from boron isotope data (i.e., δ¹¹B_{borate}) still requires independent constraints on the bulk boron isotopic composition of seawater (δ¹¹B_{SW}) as well as temperature and salinity for the purpose of calculating the borate/boric acid equilibrium constant pK_B (e.g., Zeebe & Wolf-Gladrow, 2001), which is weakly dependent also on seawater major ion composition (Hain et al., 2015) and may thus require minor correction for the deep geologic past (Henehan et al., 2016). This raises the question: Can we use boron isotope data to reconstruct CO₂ climate forcing in deep geologic time, when bulk seawater boron isotopic composition is poorly constrained and temperature reconstructions are questionable at least in their absolute sense? Or, put a different way, is the boron isotope pH proxy inherently more robust in reconstructing past pH *change* than in reconstructing *absolute* pH? To answer these questions, we first consider the established boron isotope pH proxy equation for a single sample (Zeebe & Wolf-Gladrow, 2001):

$$\text{pH}_0 = \text{pK}_B - \log_{10} \left(\frac{\delta_0 - \delta_{SW}}{\delta_{SW} - \alpha \times \delta_0 - \epsilon} \right) \quad (11)$$

where ε and α are the equilibrium boron isotope effect and fractionation factor (i.e., 27.2‰ and 1.0272; see Klochko et al., 2006), δ_{SW} is the boron isotopic composition of bulk seawater, δ₀ is the reconstructed boron isotopic composition of borate from which pH is to be calculated, and pK_B is the borate/boric acid equilibrium constant when δ₀ was formed. Accurate reconstruction of absolute pH using this formulation requires accurate reconstruction of both δ₀ and δ_{SW}, and accurate auxiliary information on absolute temperature, salinity, and seawater major ion composition to calculate pK_B. Notably, δ₀ and δ_{SW} carry equivalent weight in the established boron isotope pH proxy equation but for much of Earth history δ_{SW} is much more uncertain than reconstructions of δ₀.

To contrast the established formulation, we write the proxy equation for pH change (ΔpH) reconstructed from a set of two borate boron isotope reconstructions, δ₀ and δ₁:

$$\begin{aligned} \Delta\text{pH} &= \text{pH}_1 - \text{pH}_0 = \Delta\text{pK}_B - \log_{10} \left(\frac{\delta_1 - \delta^{11}\text{B}_{SW}}{\delta_{SW} - \alpha \times \delta_1 - \epsilon} \times \frac{\delta_{SW} - \alpha \times \delta_0 - \epsilon}{\delta_0 - \delta_{SW}} \right) \\ &= \Delta\text{pK}_B - \log_{10} \left(1 + \frac{\delta_1 - \delta_0}{\delta_{SW} - \alpha \times \delta_1 - \epsilon} \times \frac{(\alpha - 1) \times \delta_{SW} - \epsilon}{\delta_0 - \delta_{SW}} \right) \end{aligned} \quad (12)$$

While δ_{SW} is still required to calculate ΔpH, the dominant boron isotope term in the ΔpH equation is the difference between δ₁ and δ₀, which has two very significant implications. First, any error in δ_{SW} causes greater error in reconstructed pH than in ΔpH, such that ΔpH can be more accurately reconstructed than absolute pH in the face of δ_{SW} uncertainty. Second, the reconstructed values of δ₀ and δ₁ need to be precise but not necessarily accurate as long as they carry the same systematic bias (e.g., from vital effects and matrix differences between the sample material and the measurement standard), which makes the reconstruction of ΔpH inherently more robust than the reconstruction of absolute pH. Additionally, ΔpK_B only weakly depends on only relative changes in temperature, salinity, and seawater major ion composition, not absolute values, such that ΔpK_B is smaller and can be more accurately reconstructed than pK_B. Overall, our examination of the pH and ΔpH proxy equations demonstrates that reconstructions of ΔpH are both more accurate in the face of δ_{SW} uncertainty and more robust in the face of a number of potential biases than is the

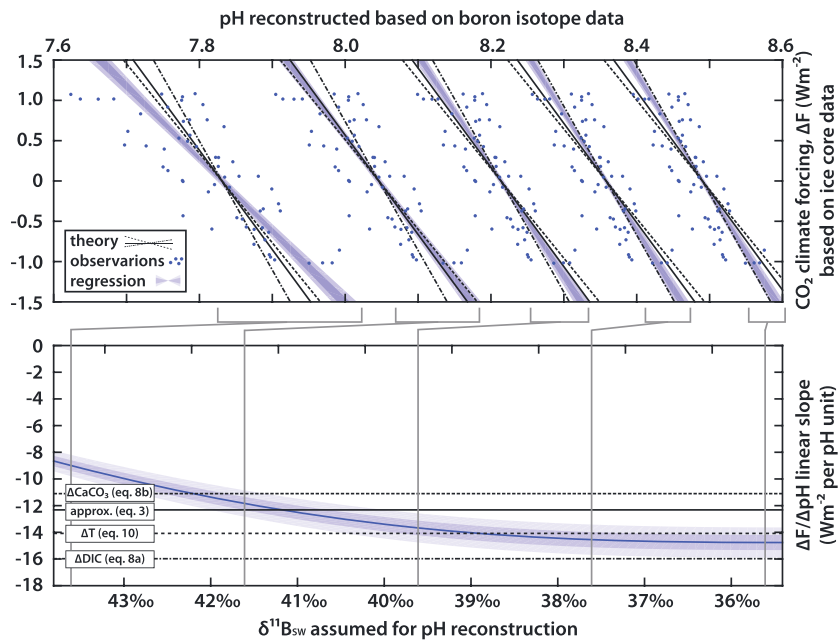


Figure 4. Relationship between ice core derived CO₂ climate forcing and ODP site 999 reconstructed pH, as in Figure 3 but this time ignoring reconstructed temperature and systematically introducing error in the seawater boron isotope composition ($\delta^{11}\text{B}_{\text{SW}}$) assumed in the pH reconstruction. The bottom panel compares observation regressed pH-CO₂ slope (blue shading) against theoretical prediction (solid and dashed black lines) as a function of systematically varied $\delta^{11}\text{B}_{\text{SW}}$. The top panel displays the observed, regressed and predicted pH-CO₂ relationship for five discrete cases: assuming true $\delta^{11}\text{B}_{\text{SW}}$ as well as deliberately introducing $\pm 2\%$ and $\pm 4\%$ error in $\delta^{11}\text{B}_{\text{SW}}$. This exercise demonstrates that reconstructed ΔpH is relatively insensitive to $\delta^{11}\text{B}_{\text{SW}}$ error, unlike absolute reconstructed pH.

reconstruction of absolute pH. We anticipate that this finding will not come as a major surprise to practitioners in the field of boron isotope geochemistry, but to our knowledge, this is the first formal statement of the fact.

Based on the above theoretical considerations, we should be able to recover the correct relationship between CO₂ climate forcing (ΔF) and pH change (ΔpH) even if we were to completely ignore temperature change (e.g., because $\Delta\text{pK}_{\text{B}}$ is only a relatively weak function of temperature change) and even if we were to deliberately introduce significant error in the bulk seawater boron isotopic composition (e.g., because δ_{SW} has little weight on the value of the logarithmic term in equation (12)). To demonstrate the pervasive differences in the reconstruction of pH and ΔpH , we turn again to the comparison of the boron isotope measurements from ODP Site 999 and the coeval ice core record of atmospheric CO₂ (as in Figure 3) but this time systematically changing the bulk seawater boron isotopic composition ($\delta^{11}\text{B}_{\text{SW}}$, same as abbreviated δ_{SW} notation in equations (11) and (12)) used in the calculation by $\pm 4.2\%$ around its true value of 39.61‰ (Figure 4). Also, we find no noticeable difference when including or excluding the effect of reconstructed local temperature changes on pK_{B} , and for the purpose of highlighting the role of δ_{SW} uncertainty we show the results where pK_{B} is taken to be constant.

As expected, the very large range of deliberately introduced offset in seawater boron isotopic composition systematically increases/decreases the mean absolute pH by more than 0.07 pH units per 1‰ of $\delta^{11}\text{B}_{\text{SW}}$ change (Figure 4a). That is, absolute pH is highly sensitive to the assumed $\delta^{11}\text{B}_{\text{SW}}$ (see also Pagani et al., 2005). In stark contrast, however, the pH range covered by the ODP Site 999 data set changes much less as $\delta^{11}\text{B}_{\text{SW}}$ is manipulated, such that the regressed $\Delta F/\Delta\text{pH}$ slope changes only mildly even in the face of substantial introduced $\delta^{11}\text{B}_{\text{SW}}$ error. Specifically, comparison of the regressed slope (blue envelope) to the relationship theoretically predicted by equation (3) suggests that the theory is a reasonably good predictor for the true ice core-derived ΔF even in the face of $\delta^{11}\text{B}_{\text{SW}}$ error as large as $\pm 2\%$ (x axis in Figure 4b), which compares favorably with the uncertainty of $\delta^{11}\text{B}_{\text{SW}}$ reported in available reconstructions (e.g., Greenop et al., 2017; Lemarchand et al., 2000; Raitzsch & Hönisch, 2013).

We note that we calculate the results shown in Figure 4 using the established pH proxy equation, and that our formulation of ΔpH (i.e., equation (12)) simply expresses the difference between two standard pH reconstructions. The main point we intend to demonstrate in this section is that $\delta^{11}\text{B}_{\text{SW}}$ uncertainty affects pH significantly more than it does ΔpH , both reconstructed using the same established boron isotope proxy equation. That is, the boron isotope proxy system inherently yields more robust estimates of past pH change than absolute pH. Earlier we showed in theory (see section 2) and observations (see section 3.1) that pH change (ΔpH) is a strong predictor for CO_2 climate forcing. In that context, our ability to obtain robust reconstructions of ΔpH from the boron isotope proxy is critical.

3.3. Climate Sensitivity

Reconstructing CO_2 radiative forcing using the boron isotope pH proxy offers important insights into the role of the global carbon cycle in causing climate change of the geologic past. However, in the context of ongoing anthropogenic climate change and when comparing different periods of geologic time the quantity of interest is often the climate sensitivity S , which is the ratio of temperature change (ΔT) per radiative climate forcing (ΔF ; e.g., Knutti & Hegerl, 2008):

$$S = \frac{\Delta T}{\Delta F} \quad (13)$$

In the case that only the component of total forcing that is due to CO_2 is explicitly considered, the climate sensitivity calculated in this way is commonly referred to as Earth System Sensitivity (ESS; Lunt et al., 2010), which implicitly includes climate system feedbacks that are *fast* (e.g., water vapor and clouds) and *slow* (e.g., dust and ice sheets). Also, there exists a spectrum of alternate definitions of climate sensitivity that explicitly include the component climate forcing of a number of these slow processes (e.g., PALEOSENS Project Members, 2012; von der Heydt et al., 2016). We note that all formulations of climate sensitivity require constraints on CO_2 climate forcing, which is the focus of our study, but detailed treatment of different types and ways to calculate climate sensitivity is beyond our scope here. That said, given the uncertainties of boron isotope measurements and the range in the ΔpH -to- ΔF conversion for different end-member causes of pH change (i.e., CaCO_3 , temperature and DIC change as described above, Figure 2), we need to address the question if our formalism can yield sufficiently accurate and precise constraints on $\Delta T/\Delta F$. To address this question, we need a target estimate of true $\Delta T/\Delta F$ and compare it to the equivalent result based on boron isotope data. For this test we again turn to the ice core CO_2 record (as compiled by Bereiter et al., 2015) to yield true CO_2 radiative forcing, which we pair with two independent reconstructions of temperature change over the late Pleistocene glacial/interglacial cycles (global mean surface air temperature MAT and SST taken from Martinez-Boti et al., 2015). We note that SST does not reflect global mean surface temperature such that using this record is not intended to yield bona fide estimates of climate sensitivity but to evaluate the accuracy and precision of our formalism in constraining climate sensitivity. Conversely, MAT is based on inverse model results of Northern Hemisphere temperature (i.e., van de Wal et al., 2011) scaled to reflect global mean surface temperature for the purpose of calculating climate sensitivity (see Martinez-Boti et al., 2015).

We interpolate the temperature records at the ages of the 1011 discrete ice core CO_2 data points of the last 260 kyr and determine $\Delta T/\Delta F$ by regressing the slope of temperature change per ice core CO_2 -derived climate forcing using the York regression method (York et al., 2004), assuming 1σ uncertainty of 1°C and 5 ppmv for temperature and ice core CO_2 , respectively. This approach yields slopes $\Delta T_{\text{MAT}}/\Delta F_{\text{ice1011}}$ of $2.5^\circ\text{C}/(\text{W}/\text{m}^2)$ and $\Delta T_{\text{SST}}/\Delta F_{\text{ice1011}}$ of $1.2^\circ\text{C}/(\text{W}/\text{m}^2)$, both with a 2σ regression slope uncertainty of $\pm 0.09^\circ\text{C}/(\text{W}/\text{m}^2)$; shown as shading in lower panel of Figure 5). That analysis, however, is not representative of $\Delta T/\Delta F$ of the last 260 kyr (for which we have boron isotope data) because uneven sampling results in almost half of the ice core derived CO_2 data points from the last 20 kyr, and more than 80% from the last 100 kyr. When we repeat the analysis but only include the ice core data that are closest to the ages of the boron isotope record (i.e., 59 samples with ~ 4 kyr sample interval), we regress $\Delta T_{\text{MAT}}/\Delta F_{\text{ice59}}$ of $2.5^\circ\text{C}/(\text{W}/\text{m}^2)$ and $\Delta T_{\text{SST}}/\Delta F_{\text{ice59}}$ of $1.3^\circ\text{C}/(\text{W}/\text{m}^2)$, both with 2σ regression slope uncertainty of $\pm 0.4^\circ\text{C}/(\text{W}/\text{m}^2)$; Figure 5; MAT and SST regressions shown in red and blue, respectively). We take these ice core CO_2 -based numbers to be the true answer in our test of the boron isotope-based reconstruction. We note that both $\Delta T_{\text{MAT}}/\Delta F_{\text{ice1011}}$ and $\Delta T_{\text{MAT}}/\Delta F_{\text{ice59}}$ are consistent with previous estimates of late Pleistocene ESS climate sensitivity to CO_2 forcing (e.g., see $S_{[\text{CO}_2]}$ in Table 2 of PALEOSENS Project Members, 2012).

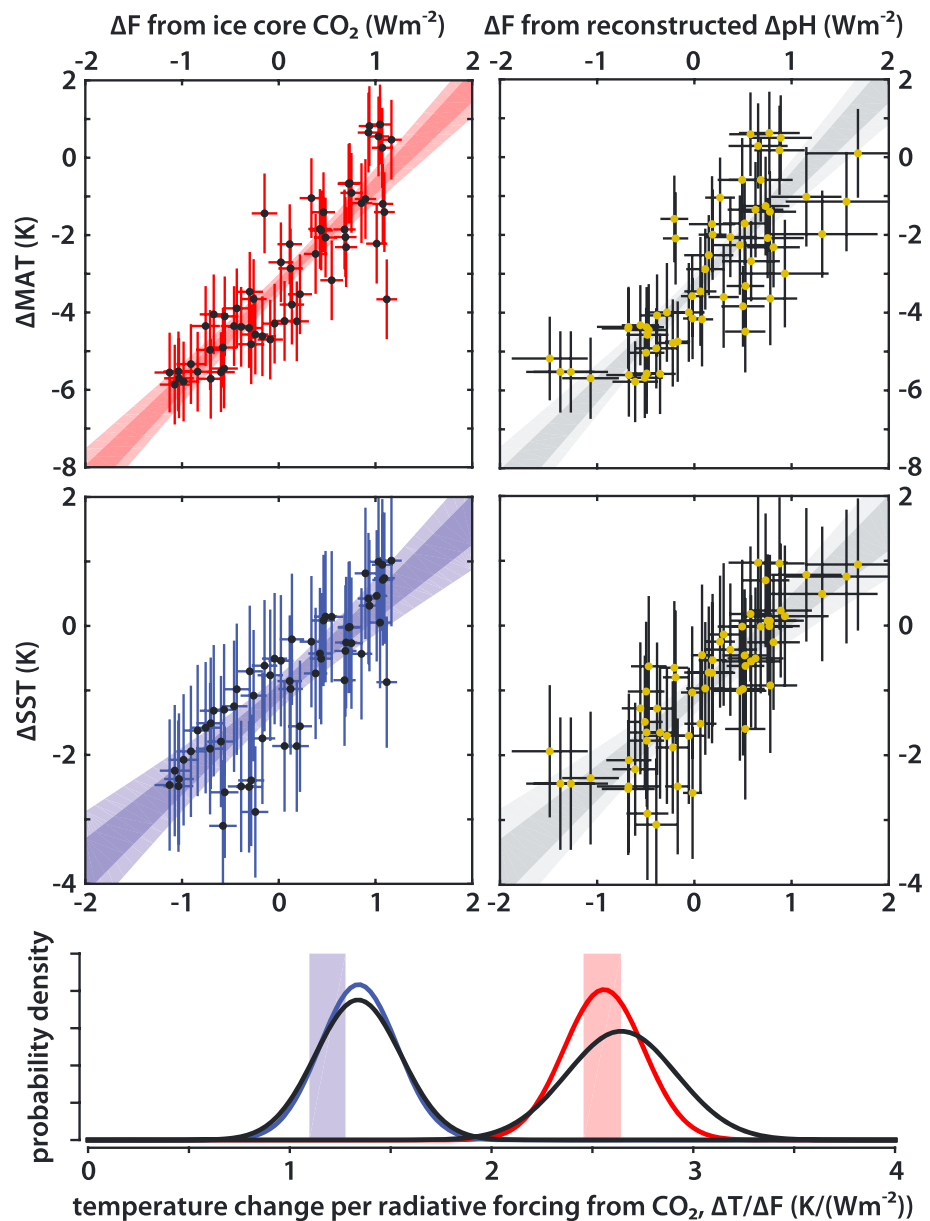


Figure 5. Regression of climate sensitivity $\Delta T/\Delta F$ based on ice core CO_2 reconstructions (red and blue) and boron isotope data (black/gray), respectively. The four square panels on the top show the regression results using two temperature records, (top) global mean surface air temperature (MAT) and (bottom) sea surface temperature (SST; see Martinez-Boti et al., 2015), side by side for the two records of climate forcing (ice core: left, and boron isotope: right), whereby the ice core data was subsampled to the ages that are closest to the 59 boron isotope data points. The bottom panel shows the probability density functions for the regressed $\Delta T/\Delta F$ slope from the above panels, compared to the regressed slope for the all ice core CO_2 data of the last 260 kyr (shading, 2σ). The standard error of ΔF determined from boron isotope data includes measurement uncertainty and the end member range of the ΔpH -to- ΔF conversion.

In determining the 2σ range of ΔF_{boron} we use the 2σ uncertainties of the boron isotope measurement of every data point conflated with the lowest and highest end-member slope of the ΔpH -to- ΔF relationship (i.e., the slope for CaCO_3 and DIC change, respectively; see Figure 2). That is, ΔF_{boron} includes the uncertainty both of the boron isotope measurement as well as the uncertainty of the conversion from ΔpH to ΔF . This treatment makes the assumption that the ΔpH -to- ΔF slope uncertainty is independent between data points, which can be justified because the reconstructed pH change of each sample is caused by a different combination of CaCO_3 , temperature, and DIC change. For the temperature data to be compared with ΔF_{boron} we

conflate the uncertainty of the temperature reconstruction (1σ of $\pm 1^\circ\text{C}$, as above) with the age uncertainty of the boron isotope data, yielding an effective temperature uncertainty only marginally larger than 1σ of $\pm 1^\circ\text{C}$. The regression based on the boron isotope data yields $T_{\text{MAT}}/\Delta F_{\text{boron}}$ of $2.6^\circ\text{C}/(\text{W}/\text{m}^2)$ with 2σ regression slope uncertainty of $\pm 0.5^\circ\text{C}/(\text{W}/\text{m}^2)$ and $\Delta T_{\text{SST}}/\Delta F_{\text{boron}}$ of $1.3^\circ\text{C}/(\text{W}/\text{m}^2)$ with 2σ of $\pm 0.4^\circ\text{C}/(\text{W}/\text{m}^2)$; shown in black in Figure 5).

Direct measurement of CO_2 on air trapped in ice cores yields inherently much more precise and accurate estimates of CO_2 climate forcing than indirect proxy-based approaches, such as the conventional application or our new formalism for the boron isotope system. Our test case illustrates that ice core-based reconstruction of $\Delta T/\Delta F$ yields more accurate and precise constraints than can be achieved based on boron isotope data, but the difference is rather modest because fractional uncertainty in temperature reconstructions is typically larger than the fractional uncertainty of the CO_2 climate forcing reconstructed based on either ice core or boron isotope data and thus dominates the uncertainty of the regressed slope $\Delta T/\Delta F$ (i.e., fractional uncertainty referring to the ratio of uncertainty to the overall recorded signal). That is, our test suggests that boron isotope data can in principle be used to reconstruct climate sensitivity with an uncertainty not substantially larger than based on ice core CO_2 data, when the number of data points is the same. More precise constraints on temperature change and more discrete data points are best suited to reduce the uncertainty of the regressed climate sensitivity, rather than further reducing the uncertainty in reconstructed CO_2 climate forcing. We highlight that our formalism yields adequate constraints on climate forcing without requiring any assumption of a second carbonate system parameter, without knowledge of the carbonate chemistry equilibrium constants (i.e., $\text{p}K_0$, $\text{p}K_1$, and $\text{p}K_2$; which are strongly dependent on temperature and the major ion composition of seawater), and without highly precise knowledge of the boron isotopic composition of seawater ($\delta^{11}\text{B}_{\text{SW}}$). Contrary to the conventional application of the boron isotope system, our formalism yields adequate constraints on climate sensitivity using only the boron isotope data, reconstructed local temperature change (to calculate $\Delta\text{p}K_{\text{B}}$ for the ΔpH reconstruction, which is a weak function of relative temperature change), and best guess $\delta^{11}\text{B}_{\text{SW}}$ (see section 3.4 and Figure 4), all of which can be obtained from the geologic record significantly older than the reach of ice cores.

4. Discussion and Caveats

The boron isotope pH proxy is firmly established as a tool to reconstruct past ocean pH (e.g., Foster & Rae, 2016; Hemming & Hönisch, 2007; Rae et al., 2011; Zeebe & Wolf-Gladrow, 2001), and its usage to place constraints on past ocean acid/base chemistry is rapidly increasing. Furthermore, if the sample material originates from the highly stratified and close to air/sea equilibrated subtropical surface, with auxiliary constraints on ambient temperature and an assumption on a second carbonate system parameter (such as DIC and alkalinity), the boron isotope pH proxy is routinely extended to reconstruct past atmospheric CO_2 and its radiative forcing of climate change. It is well established (e.g., Greenop et al., 2017; Pearson & Palmer, 2000; Raitzsch & Hönisch, 2013) that this conventional approach relies heavily on accurate and independent knowledge of past seawater boron isotopic composition ($\delta^{11}\text{B}_{\text{SW}}$) and on the (explicitly or implicitly) assumed seawater carbon content (DIC), alkalinity (ALK), or CaCO_3 saturation state. Beyond the last few million years of Earth history, both $\delta^{11}\text{B}_{\text{SW}}$ and these second carbonate system parameters are poorly known, thereby stifling the use of the boron isotope proxy system to investigate the role of the global carbon cycle in forcing climate change throughout most of geologic time. With this paper we hope to lay the groundwork for the robust application of the boron isotope proxy system for geologic periods when $\delta^{11}\text{B}_{\text{SW}}$, a second carbonate system parameter such as DIC, and/or absolute temperature cannot be determined with the previously required degree of accuracy.

In this study we propose three main new concepts to extend the utility of the boron isotope proxy system, respectively relating to (1) $\delta^{11}\text{B}_{\text{SW}}$, (2) the need for a second carbonate system parameter, and (3) the role of temperature change via its effect on carbonate chemistry equilibrium constants and Henry's law.

First, we demonstrate that when $\delta^{11}\text{B}_{\text{SW}}$ is poorly constrained the boron isotope proxy system can be used to robustly reconstruct ΔpH , but not absolute pH (Figure 3). This result is firmly based in first principle theory. We caution, however, that this approach is only applicable to boron isotope time series that cover no more than a few million years because it assumes that $\delta^{11}\text{B}_{\text{SW}}$ is constant within the data set. This timescale is

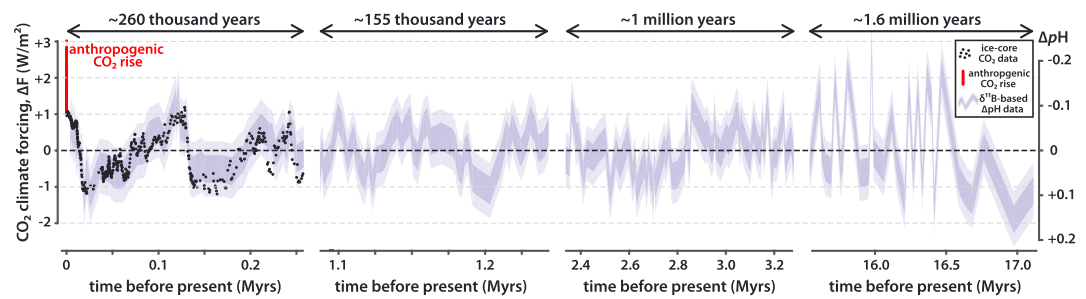


Figure 6. Reconstruction of CO₂ climate forcing using equations (3) and (6a)–(6d), based on Pleistocene, Plio-Pleistocene, and mid-Miocene boron isotope records of Chalk et al. (2017), Martinez-Boti et al. (2015), and Greenop et al. (2014), respectively, with uncertainty envelope determined empirically from the offset to CO₂ climate forcing calculated from ice core data (black dots). This new approach for reconstructing CO₂ climate forcing requires no assumption for a second carbon chemistry parameter and is relatively insensitive to error in $\delta^{11}\text{B}_{\text{SW}}$. Our formalism quantifies orbital-timescale CO₂ climate forcing but not long-term changes such as between the different data sets or trends within the longer Plio-Pleistocene and Miocene data sets. That is, the conversion from ΔpH (right axis) to climate forcing (left axis) according to equation (3) is only valid for records that are shorter than the carbon residence time.

fundamentally set by the ocean residence time of boron, which is canonically assumed to be 10–20 million years (Lemarchand et al., 2002) but may be somewhat shorter (Greenop et al., 2017).

Second, we demonstrate that that CO₂ climate forcing (ΔF) and its causal fractional CO₂ change ($\Delta\log\text{CO}_2$) are tightly related to pH change (ΔpH) and fractional change in bicarbonate and DIC (i.e., $\Delta\log\text{HCO}_3^-$ and $\Delta\log\text{DIC}$). We argue that both $\Delta\log\text{HCO}_3^-$ and $\Delta\log\text{DIC}$ must be relatively small on timescales shorter than the oceans residence time of carbon with respect to the geologic CO₂ sources and silicate weathering (very roughly 1 million years), such that ΔpH is the overwhelmingly dominant driver of atmospheric CO₂ change and its climate forcing on orbital timescales. That is, even at times when absolute DIC is unknown, we argue it is fair to assume that $\Delta\log\text{DIC}$ and $\Delta\log\text{HCO}_3^-$ are small compared to ΔpH reconstructed from a boron isotope data set that spans no more than a few orbital cycles, akin to the late Pleistocene ice age CO₂ cycles that we use to validate our formalism. We caution that relaxing the DIC constraint in this way does not apply to events of abrupt carbon addition in secular steady state with carbonate compensation (i.e., the Paleocene-Eocene thermal maximum), in which case $\Delta\log\text{DIC}$ could significantly contribute to ΔF and relying on ΔpH alone would underestimate ΔF .

Third, while temperature significantly affects both the conventional boron isotope pH proxy and the partitioning of carbon between the atmosphere and seawater, we show that it has a surprisingly weak effect on the relationship between the range of boron isotope measurements in a given data set, the ΔpH reconstructed from this data, and on the climate forcing ΔF inferred from it. To be clear, any information on temperature change will improve reconstructed ΔpH and ΔF because it constrains the presumably small ΔpK terms in equations (2a)–(2d) and (12). To achieve these improvements requires only accurate information on temperature differentials (i.e., temperature information needs to be precise but can be inaccurate) such that accurate information on absolute temperatures is not required. This insight is very convenient even if it is the completely coincidental result of the approximately linear temperature dependence of the pK equilibrium constants (i.e., the exponential temperature dependence of the equilibrium constants K ; $\text{pK} = -\log K$).

Considering the advantages and caveats outlined above, how can our new approach be used to make useful inferences about past CO₂ climate forcing? And what type of boron isotope sampling strategy is best suited to recover robust reconstructions of CO₂ climate forcing? To illustrate and discuss these questions, we apply our formalism to four boron isotope data sets (Figure 6): the orbitally resolved record of the intensification of northern hemispheric glaciation at the Plio-Pleistocene transition by Martinez-Boti et al. (2015), the record across the Middle Miocene Climatic Optimum (MMCO) by Greenop et al. (2014) that exhibits but does not fully resolve, orbital-timescale boron isotope changes, and the new highly resolved late and mid Pleistocene records from ODP Site 999 (Chalk et al., 2017), the former of which we used to validate our formalism.

All these records are short relative to the residence time of boron in the ocean, which precludes significant change in $\delta^{11}\text{B}_{\text{SW}}$ over the duration of each time slice. Thus, we use modern $\delta^{11}\text{B}_{\text{SW}}$ for the Plio-

Pleistocene data (39.61‰; Foster et al., 2010), and a lower $\delta^{11}\text{B}_{\text{SW}}$ value of 37.82‰ for the mid-Miocene (Foster et al., 2012; Greenop et al., 2014). As we demonstrate here (e.g., Figure 4), using slightly different estimates for low mid-Miocene $\delta^{11}\text{B}_{\text{SW}}$ (e.g., Lemarchand et al., 2002; Greenop et al., 2017; Raitzsch & Hönisch, 2013) would make no significant difference because pH change reconstruction is much less sensitive to the $\delta^{11}\text{B}_{\text{SW}}$ value than is the reconstruction of absolute pH. For all data sets we calculate ΔpH relative to the average $\delta^{11}\text{B}_{\text{borate}}$ and relative to the average reconstructed temperature of the respective data set, using equation (12) without approximation. Hence, we can plot the data on the same axes of pH change and CO_2 climate forcing, but this axis only applies to changes within each respective data set and not to changes between them.

The residence time of carbon relative to total weathering is about 200 thousand years but only a fraction of total weathering is due to silicate weathering, such that fractional change of ocean DIC can be assumed to be small on a roughly million-year timescale and shorter. Hence, we cannot quantify a likely small contribution of DIC change (i.e., $\Delta\log\text{HCO}_3^-$) to climate forcing, for example, at the onset of the MMCO at 17.2–16.5 Myr or across the duration of the Plio-Pleistocene time slice at 3.3–2.3 Myr. However, the orbital-timescale changes evident in all three data sets, as well as the abrupt ~ 2.8 Myr step change associated with the intensification of Northern Hemisphere glaciation, are too rapid to allow for significant DIC change and must therefore satisfy our formalism, as is supported by the good agreement with the ice core CO_2 data (Figures 3 and 6). As a caution, the orbital-timescale fluctuations during the MMCO are not fully resolved, often supported only by single low- $\delta^{11}\text{B}$ data points and thus prone to be questioned as being outliers. In this context, using a boron isotope record that is sufficiently resolved to support orbital-timescale $\delta^{11}\text{B}_{\text{borate}}$ fluctuations with multiple data points is prudent when aiming to reconstruct climate forcing.

Based on these considerations, we argue that data sets that fully resolve orbital timescales over the course of time slices not significantly longer than about 1 million years are most suited for the reconstruction of pH change and CO_2 climate forcing. To the best of our knowledge, such data sets are exceedingly rare at the moment, with most efforts currently aimed at generating long-term, low-resolution records that require highly uncertain corrections for $\delta^{11}\text{B}_{\text{SW}}$ and DIC change to reconstruct CO_2 climate forcing. In the absence of detailed constraints on $\delta^{11}\text{B}_{\text{SW}}$ and a second carbonate system parameter (e.g., DIC), we argue that only a sampling strategy that targets relatively abrupt transitions or orbital cyclicity can yield robust quantification of pH change and the associated CO_2 climate forcing. Furthermore, samples should be taken from low-latitude open-ocean sites that are close to CO_2 equilibrium with the atmosphere, and exclude time intervals with known biogeochemical aberrations (such as widespread anoxia or euxinia) that may violate our formalism. With these caveats, we demonstrate that boron isotope data can yield adequate constraints on CO_2 climate forcing.

Ultimately, we hope the formalism, theory, and validation presented in this study opens the door to utilize the boron isotope proxy system to derive quantitative constraints on the various types of climate sensitivity (e.g., Equilibrium Climate Sensitivity, Earth System Sensitivity; cf. Lunt et al., 2010; PALEOSENS Project Members, 2012). Combined with independent climate reconstructions and ice sheet modeling (e.g., Köhler et al., 2015; PALEOSENS Project Members, 2012; Royer et al., 2016), these constraints will enable the mapping out of changes in ESS and ECS (e.g., Köhler et al., 2015; von der Heydt et al., 2016) as the planet transitioned from the early Cenozoic greenhouse to the recurring Pleistocene ice ages, improving our understanding of our planet's climate machine as well as honing projections of its future under continued anthropogenic perturbation.

Acknowledgments

We thank Sarah Greene, an unnamed referee, and the Associate Editor for helpful comments and suggestions. This study was supported by UK Natural Environment Research Council grants NE/K00901X/1 to M. P. H., NE/I006346/1 to G. L. F., NE/P011381/1 to G. L. F. and M. P. H., and NE/I528626/1 to T. C. The Pleistocene boron isotope data can be found at <https://doi.pangaea.de/10.1594/PANGAEA.882551>.

References

- Andrews, T., Gregory, J. M., Webb, M. J., & Taylor, K. E. (2012). Forcing, feedbacks and climate sensitivity in CMIP5 coupled atmosphere–ocean climate models. *Geophysical Research Letters*, *39*, L09712. <https://doi.org/10.1029/2012GL051607>
- Bereiter, B., Eggleston, S., Schmitt, J., Nehrbass-Ahles, C., Stocker, T., Fischer, H., et al. (2015). Revision of the EPICA Dome C CO_2 record from 800 to 600kyr before present. *Geophysical Research Letters*, *42*, 542–549. <https://doi.org/10.1002/2014GL061957>
- Breecker, D., Sharp, Z., & McFadden, L. (2010). Atmospheric CO_2 concentrations during ancient greenhouse climates were similar to those predicted for AD 2100. *Proceedings of the National Academy of Sciences of the United States of America*, *107*(2), 576–580. <https://doi.org/10.1073/pnas.0902323106>
- Broecker, W. S., & Peng, T.-H. (1987). The role of CaCO_3 compensation in the glacial to interglacial atmospheric CO_2 change. *Global Biogeochemical Cycles*, *1*, 15–29. <https://doi.org/10.1029/GB001i001p00015>

- Byrne, B., & Goldblatt, C. (2014). Radiative forcing at high concentrations of well-mixed greenhouse gases. *Geophysical Research Letters*, *41*, 152–160. <https://doi.org/10.1002/2013GL058456>
- Chalk, T. B., Hain, M. P., Foster, G. L., Rohling, E. J., Sexton, P. F., Badger, M. P. S., et al. (2017). Causes of ice age intensification across the mid-Pleistocene transition. *Proceedings of the National Academy of Sciences of the United States of America*, *114*(50), 13,114–13,119. <https://doi.org/10.1073/pnas.1702143114>
- Foster, G. (2008). Seawater pH, PCO₂ and [CO₃²⁻] variations in the Caribbean Sea over the last 130 kyr: A boron isotope and B/Ca study of planktic foraminifera. *Earth and Planetary Science Letters*, *271*(1–4), 254–266. <https://doi.org/10.1016/j.epsl.2008.04.015>
- Foster, G., Honisch, B., Paris, G., Dwyer, G., Rae, J., Elliott, T., et al. (2013). Interlaboratory comparison of boron isotope analyses of boric acid, seawater and marine CaCO₃ by MC-ICPMS and NTIMS. *Chemical Geology*, *358*, 1–14. <https://doi.org/10.1016/j.chemgeo.2013.08.027>
- Foster, G., Lear, C., & Rae, J. (2012). The evolution of pCO₂, ice volume and climate during the middle Miocene. *Earth and Planetary Science Letters*, *341*, 243–254.
- Foster, G., Pogge von Strandmann, P., & Rae, J. (2010). Boron and magnesium isotopic composition of seawater. *Geochemistry, Geophysics, Geosystems*, *11*, Q08015. <https://doi.org/10.1029/2010GC003201>
- Foster, G. L., & Rae, J. W. B. (2016). Reconstructing ocean pH with boron isotopes in foraminifera. *Annual Review of Earth and Planetary Sciences*, *44*(1), 207–237. <https://doi.org/10.1146/annurev-earth-060115-012226>
- Franks, P., Royer, D., Beerling, D., Van de Water, P., Cantrill, D., Barbour, M., & Berry, J. (2014). New constraints on atmospheric CO₂ concentration for the Phanerozoic. *Geophysical Research Letters*, *41*, 4685–4694. <https://doi.org/10.1002/2014GL060457>
- Goodwin, P., Katavouta, A., Roussenov, V. M., Foster, G. L., Rohling, E. J., & Williams, R. G. (2018). Pathways to 1.5 degrees C and 2 degrees C warming based on observational and geological constraints. *Nature Geoscience*, *11*(2), 102.
- Greenop, R., Foster, G., Wilson, P., & Lear, C. (2014). Middle Miocene climate instability associated with high-amplitude CO₂ variability. *Paleoceanography*, *29*, 845–853. <https://doi.org/10.1002/2014PA002653>
- Greenop, R., Hain, M., Sosdian, S., Oliver, K., Goodwin, P., Chalk, T., et al. (2017). A record of Neogene seawater delta B-11 reconstructed from paired delta B-11 analyses on benthic and planktic foraminifera. *Climate of the Past*, *13*(2), 149–170. <https://doi.org/10.5194/cp-13-149-2017>
- Hain, M., Sigman, D., & Haug, G. (2010). Carbon dioxide effects of Antarctic stratification, North Atlantic Intermediate Water formation, and subantarctic nutrient drawdown during the last ice age: Diagnosis and synthesis in a geochemical box model. *Global Biogeochemical Cycles*, *24*, GB4023. <https://doi.org/10.1029/2010GB003790>
- Hain, M., Sigman, D., Higgins, J., & Haug, G. (2015). The effects of secular calcium and magnesium concentration changes on the thermodynamics of seawater acid/base chemistry: Implications for Eocene and Cretaceous ocean carbon chemistry and buffering. *Global Biogeochemical Cycles*, *29*, 517–533. <https://doi.org/10.1002/2014GB004986>
- Hain, M. P., Sigman, D. M., & Haug, G. H. (2014). The biological pump in the past. In *The oceans and marine geochemistry, Treatise on geochemistry* (2nd ed., Vol. 8, pp. 485–517). Amsterdam: Elsevier.
- Hemming, N., & Hanson, G. (1992). Boron isotopic composition and concentration in modern marine carbonates. *Geochimica et Cosmochimica Acta*, *56*(1), 537–543. [https://doi.org/10.1016/0016-7037\(92\)90151-8](https://doi.org/10.1016/0016-7037(92)90151-8)
- Hemming, N. G., & Hönisch, B. (2007). Boron isotopes in marine carbonate sediments and the pH of the ocean. In M. C. Hillaire & A. DeVernal (Eds.), *Proxies in Late Cenozoic paleoceanography, Developments in marine geology* (pp. 717–734). Amsterdam, Netherlands: Elsevier.
- Henehan, M., Hull, P., Penman, D., Rae, J., & Schmidt, D. (2016). Biogeochemical significance of pelagic ecosystem function: An end-Cretaceous case study. *Philosophical Transactions of the Royal Society, B: Biological Sciences*, *371*(1694). <https://doi.org/10.1098/rstb.2015.0510>
- IPCC (2014). *Climate change 2014: Synthesis report*. Contribution of working groups I, II and III to the Fifth Assessment Report of the Intergovernmental Panel on Climate Change, [Core Writing Team, R.K. Pachauri and L.A. Meyer (eds.)]. IPCC, Geneva, Switzerland, 151 pp.
- Klochko, K., Kaufman, A. J., Yao, W., Byrne, R. H., & Tossell, J. A. (2006). Experimental measurement of boron isotope fractionation in seawater. *Earth and Planetary Science Letters*, *248*(1–2), 276–285. <https://doi.org/10.1016/j.epsl.2006.05.034>
- Knutti, R., & Hegerl, G. C. (2008). The equilibrium sensitivity of the Earth's temperature to radiation changes. *Nature Geoscience*, *1*(11), 735–743. <https://doi.org/10.1038/ngeo337>
- Knutti, R., Rugenstein, M. A. A., & Hegerl, G. C. (2017). Beyond equilibrium climate sensitivity. *Nature Geoscience*, *10*(10), 727.
- Köhler, P., de Boer, B., von der Heydt, A., Stap, L., & van de Wal, R. (2015). On the state dependency of the equilibrium climate sensitivity during the last 5 million years. *Climate of the Past*, *11*(12), 1801–1823. <https://doi.org/10.5194/cp-11-1801-2015>
- Lemarchand, D., Gaillardet, J., Lewin, E., & Allegre, C. (2000). The influence of rivers on marine boron isotopes and implications for reconstructing past ocean pH. *Nature*, *408*(6815), 951–954. <https://doi.org/10.1038/35050058>
- Lemarchand, D., Gaillardet, J., Lewin, E., & Allegre, C. (2002). Boron isotope systematics in large rivers: Implications for the marine boron budget and paleo-pH reconstruction over the Cenozoic. *Chemical Geology*, *190*(1–4), 123–140. [https://doi.org/10.1016/S0009-2541\(02\)00114-6](https://doi.org/10.1016/S0009-2541(02)00114-6)
- Lunt, D., Haywood, A., Schmidt, G., Salzmann, U., Valdes, P., & Dowsett, H. (2010). Earth system sensitivity inferred from Pliocene modelling and data. *Nature Geoscience*, *3*(1), 60–64. <https://doi.org/10.1038/ngeo706>
- Martinez-Boti, M., Foster, G., Chalk, T., Rohling, E., Sexton, P., Lunt, D., et al. (2015). Plio-Pleistocene climate sensitivity evaluated using high-resolution CO₂ records. *Nature*, *518*(7537), 49.
- Martinez-Garcia, A., Sigman, D., Ren, H., Anderson, R., Straub, M., Hodell, D., et al. (2014). Iron fertilization of the subantarctic ocean during the last ice age. *Science*, *343*(6177), 1347–1350. <https://doi.org/10.1126/science.1246848>
- Myhre, G., Highwood, E., Shine, K., & Stordal, F. (1998). New estimates of radiative forcing due to well mixed greenhouse gases. *Geophysical Research Letters*, *25*, 2715–2718. <https://doi.org/10.1029/98GL01908>
- Pagani, M. (2014). *Biomarker-based inferences of past climate: The alkenone pCO₂ proxy*, *Treatise on geochemistry* (2nd ed. pp. 361–378). Oxford: Elsevier.
- Pagani, M., Lemarchand, D., Spivack, A., & Gaillardet, J. (2005). A critical evaluation of the boron isotope-pH proxy: The accuracy of ancient ocean pH estimates. *Geochimica et Cosmochimica Acta*, *69*(4), 953–961. <https://doi.org/10.1016/j.gca.2004.07.029>
- PALEOSENS Project Members (2012). Making sense of palaeoclimate sensitivity. *Nature*, *491*(7426), 683–691. <https://doi.org/10.1038/nature11574>
- Pearson, P., & Palmer, M. (2000). Atmospheric carbon dioxide concentrations over the past 60 million years. *Nature*, *406*(6797), 695–699. <https://doi.org/10.1038/35021000>
- Rae, J., Foster, G., Schmidt, D., & Elliott, T. (2011). Boron isotopes and B/Ca in benthic foraminifera: Proxies for the deep ocean carbonate system. *Earth and Planetary Science Letters*, *302*(3–4), 403–413. <https://doi.org/10.1016/j.epsl.2010.12.034>

- Raitzsch, M., & Hönisch, B. (2013). Cenozoic boron isotope variations in benthic foraminifers. *Geology*, *41*(5), 591–594. <https://doi.org/10.1130/G34031.1>
- Rodenbeck, C., Keeling, R., Bakker, D., Metz, N., Olsen, A., Sabine, C., & Heimann, M. (2013). Global surface-ocean $p(\text{CO}_2)$ and sea-air CO_2 flux variability from an observation-driven ocean mixed-layer scheme. *Ocean Science*, *9*(2), 193–216. <https://doi.org/10.5194/os-9-193-2013>
- Rohling, E. J., Marino, G., Foster, G. L., Goodwin, P. A., von der Heydt, A. S., & Koehler, P. (2018). Comparing climate sensitivity, past and present. *Annual Review of Marine Science*, *10*(10), 261.
- Royer, D. (2006). CO_2 -forced climate thresholds during the Phanerozoic. *Geochimica et Cosmochimica Acta*, *70*(23), 5665–5675. <https://doi.org/10.1016/j.gca.2005.11.031>
- Royer, D., Jeanloz, R., & Freeman, K. (2016). Climate sensitivity in the geologic past. *Annual Review of Earth and Planetary Sciences*, *44*(1), 277–293. <https://doi.org/10.1146/annurev-earth-100815-024150>
- Shakun, J. D., Clark, P. U., He, F., Marcott, S. A., Mix, A. C., Liu, Z., et al. (2012). Global warming preceded by increasing carbon dioxide concentrations during the last deglaciation. *Nature*, *484*(7392), 49–54. <https://doi.org/10.1038/nature10915>
- Sigman, D., & Boyle, E. (2000). Glacial/interglacial variations in atmospheric carbon dioxide. *Nature*, *407*(6806), 859–869. <https://doi.org/10.1038/35038000>
- Sigman, D., Hain, M., & Haug, G. (2010). The polar ocean and glacial cycles in atmospheric CO_2 concentration. *Nature*, *466*(7302), 47–55. <https://doi.org/10.1038/nature09149>
- Spivack, A., & Edmond, J. (1987). Boron isotope exchange between seawater and the oceanic-crust. *Geochimica et Cosmochimica Acta*, *51*(5), 1033–1043. [https://doi.org/10.1016/0016-7037\(87\)90198-0](https://doi.org/10.1016/0016-7037(87)90198-0)
- Spivack, A., You, C., & Smith, H. (1993). Foraminiferal boron isotope ratios as a proxy for surface ocean pH over the past 21-Myr. *Nature*, *363*(6425), 149–151. <https://doi.org/10.1038/363149a0>
- Takahashi, T., Sutherland, S. C., Sweeney, C., Poisson, A., Metz, N., Tilbrook, B., et al. (2002). Global sea-air CO_2 flux based on climatological surface ocean $p\text{CO}_2$, and seasonal biological and temperature effects. *Deep-Sea Research Part II-Topical Studies in Oceanography*, *49*(9–10), 1601–1622. [https://doi.org/10.1016/S0967-0645\(02\)00003-6](https://doi.org/10.1016/S0967-0645(02)00003-6)
- Takahashi, T., Sutherland, S. C., Wanninkhof, R., Sweeney, C., Feely, R. A., Chipman, D. W., et al. (2009). Climatological mean and decadal change in surface ocean $p\text{CO}_2$, and net sea-air CO_2 flux over the global oceans. *Deep-Sea Research Part II-Topical Studies in Oceanography*, *56*(8–10), 554–577. <https://doi.org/10.1016/j.dsr2.2008.12.009>
- Toggweiler, J. R. (1999). Variation of atmospheric CO_2 by ventilation of the ocean's deepest water. *Paleoceanography*, *14*(5), 571–588. <https://doi.org/10.1029/1999PA900033>
- van de Wal, R. S. W., de Boer, B., Lourens, L. J., Koehler, P., & Bintanja, R. (2011). Reconstruction of a continuous high-resolution CO_2 record over the past 20 million years. *Climate of the Past*, *7*(4), 1459–1469.
- von der Heydt, A. S., Dijkstra, H. A., van de Wal, R. S. W., Caballero, R., Crucifix, M., Foster, G. L., et al. (2016). Lessons on climate sensitivity from past climate changes. *Current Climate Change Reports*, *2*(4), 148–158. <https://doi.org/10.1007/s40641-016-0049-3>
- Vengosh, A., Kolodny, Y., Starinsky, A., Chivas, A., & McCulloch, M. (1991). Coprecipitation and isotopic fractionation of boron in modern biogenic carbonates. *Geochimica et Cosmochimica Acta*, *55*(10), 2901–2910. [https://doi.org/10.1016/0016-7037\(91\)90455-E](https://doi.org/10.1016/0016-7037(91)90455-E)
- Wang, X., Sigman, D. M., Prokopenko, M. G., Adkins, J. F., Robinson, L. F., Hines, S. K., et al. (2017). Deep-sea coral evidence for lower Southern Ocean surface nitrate concentrations during the last ice age. *Proceedings of the National Academy of Sciences of the United States of America*, *114*(13), 3352–3357. <https://doi.org/10.1073/pnas.1615718114>
- York, D., Evensen, N. M., Martinez, M. L., & Delgado, J. D. (2004). Unified equations for the slope, intercept, and standard errors of the best straight line. *American Journal of Physics*, *72*(3), 367–375. <https://doi.org/10.1119/1.1632486>
- Zachos, J. C., Dickens, G. R., & Zeebe, R. E. (2008). An early Cenozoic perspective on greenhouse warming and carbon-cycle dynamics. *Nature*, *451*(7176), 279–283. <https://doi.org/10.1038/nature06588>
- Zeebe, R. E., & Wolf-Gladrow, D. (2001). Stable isotope fractionation. In *CO_2 in seawater: Equilibrium, kinetics, isotopes* (pp. 141–250). Amsterdam: Elsevier.